SCAL Workflow for Heterogeneous Pre-salt Carbonate Rocks

Ying Gao[1,*], *Tibi* Sorop[1], *Hilbert* van der Linde[1], *Fons* Marcelis[1], *Niels* Brussee[1], *Santiago* Drexler[2], *and Yingxue* Wang[3]

[1] Shell Global Solutions International B.V., 1103 HW Amsterdam, Netherlands
[2] Shell Brasil Petroleo Ltda., Rio de Janeiro, Brazil
[3] Shell Exploration & Production Company, Houston, Texas, USA

Abstract. Pre-salt carbonates are amongst the most relevant reservoirs in Brazil. The reservoirs are highly heterogeneous, with large variations in porosity and permeability and often contain significant amounts of solid hydrocarbons inside the pores or on the pore throats, all of these making it challenging to properly describe the reservoirs. Moreover, the complexity of the fluids, often rich in light components, adds to the difficulty of accurately estimating reserves and forecasting production or to selection of the most optimal production strategy. In our view, Advanced Special Core Analysis (SCAL) techniques and integrated workflows are necessary for a better understanding on how these complexities impact the recovery process and the production strategies. In the Shell Rocks & Fluids laboratory in Amsterdam, we combined innovative technologies, including imaging with μCT, NMR/MRI, SEM, etc. with coreflooding performed using in-situ saturation monitoring (ISSM), to obtain reliable fluid flow parameters such as relative permeability, capillary pressure, trapping properties for these challenging carbonates. In this article, we provide a detailed description of the integrated SCAL workflow used for the pre-salt carbonate rocks. This includes careful selection of the samples for SCAL tests, characterization using a multitude of techniques, a research study on selecting the most optimal solvent for effective cleaning (while preserving the integrity of the reservoir rock, including of solid hydrocarbons), as well as an assessment on how heterogeneity impacts the interpretation of coreflooding tests used to extract relative permeabilities. The X-ray based ISSM played a key role in execution and interpretation of the steady-state coreflooding tests (for water-oil displacing process) and the unsteady state coreflooding tests (for water-gas displacement). Multispeed centrifuge tests were performed in parallel to obtain imbibition capillary pressure. All experimental tests were history matched using in-house numerical simulations techniques, in order to accurately interpret the results, and to extract reliable input parameters for further upscaling to the static and dynamic models used for field development plans of pre-salt carbonates portfolio.

1. Introduction

Pre-salt carbonate reservoirs, mainly located offshore Brazil, have garnered significant attention due to their substantial hydrocarbon potential. The pre-salt reservoirs are primarily composed of carbonates, such as limestone and dolomite, which were deposited in a lacustrine environment. These reservoirs represent a significant opportunity for the oil and gas industry. Their discovery has significantly boosted Brazil's oil reserves, making it one of the leading oil producers globally [1,2,3,4,5].

These reservoirs are characterized by their complex geological structures and unique formation processes. The depositional environment, diagenetic processes, and tectonic activities have resulted in a highly variable reservoir architecture and properties. The heterogeneity has been observed in pre-salt formations at different scales. It affects both connectivity and fluid distribution at sector to reservoir scale, and porosity and permeability at smaller scale. Characterizing and modelling this heterogeneity is crucial for effective reservoir management, credible production forecast, and optimal hydrocarbon recovery. Traditionally, core-plug-based porosity and permeability provides key inputs to the reservoir characterization. In core analysis, homogenous samples are used for testing and one-dimensional (1D) numerical models are used in data interpretation. Heterogeneity is captured by a sample selection scheme that covers different rock types [6,7] and/or in field scale reservoir modelling. Pre-salt cores exhibit heterogeneity at finer scale. The variability in properties present at core-plug scale challenges the assumption of homogeneity we often use in core analysis and interpretation.

The recovery mechanisms for those offshore pre-salt fields include water floods, gas floods, and Water-Alternating-Gas (WAG) injection [3,4,5,8]. Special Core Analysis (SCAL) data including capillary pressure and relative permeability are key to properly model the hydrocarbon distribution, the multiphase displacement,

* Corresponding author: Y.Gao3@shell.com

and the recovery process. They are also the basis for complicated trapping and hysteresis evaluation. To our knowledge, although some notable articles have been published already [3,4,6,8], there is limited relative permeability data of pre-salt carbonates available in literature. The challenging nature of the reservoir rocks and fluids could have contributed to it.

Similar to the above-mentioned porosity and permeability characterization, in a traditional SCAL experimental program, homogeneous core plug samples are used to obtain relative permeability and capillary pressure information. With the heterogeneity observed at the core plug scale, it is important to assess if we can use 1D numerical models in the interpretation to derive credible SCAL data. In cases where detailed local porosity and permeability are needed to model the fluid flow, three-dimensional numerical models would be required [6,9]. 1D interpretation can still be used in data QAQC and to identify impacts of heterogeneity. In 1D interpretation, the core sample is assumed to be homogeneous, and the capillary end-effect (Pc-end effect) drives the saturation profiles along the sample. For a heterogeneous core sample, both Pc end-effect and the heterogeneity impact the saturation distribution. Depending on the interplay between the capillarity and the local heterogeneity, saturation profiles along the sample can fluctuate beyond the normal X-ray noise level and show gradients towards the outlet. By assessing the impact of capillary pressure using 1D interpretation, one can identify the impacts of heterogeneity.

In addition to the complex pore structures, the fluids within pre-salt carbonate reservoirs add another layer of complexity. The fluids in these reservoirs are often rich in light components, such as methane, ethane, and other light hydrocarbons. These light components are less likely to change the rock surface towards oil wetness. However, in general, carbonate reservoirs often displaying oil-wet behavior, which is associated with the polar (e.g. acidic and natural asphaltenic) components that adhere on carbonate rocks and change wettability. This implies that the interaction between the rock surface and the fluid phases must be carefully studied and understood (see also [10]). This is especially the case for reservoirs which contain significant amounts of solid hydrocarbons inside the pores or on the pore throats, which can also have a significant impact on wettability.

The combination of all these factors requires, in our view, advanced technologies and innovative approaches to accurately handle, clean, characterize and prepare samples for analyses. Advanced SCAL techniques, including imaging with Micro-Computer Tomography (mCT), Nuclear Magnetic Resonance (NMR)/Magnetic Resonance Imaging (MRI), Scanning Electron Microscopy (SEM), coreflooding performed using in-situ saturation monitoring (ISSM) [11], and integrated workflows between SCAL, PVT and geochemistry are necessary to achieve reliable results.

2. Experimental Program

An integrated SCAL program was recently carried out at the Shell Rocks & Fluids Laboratory in Energy Transition Center Amsterdam (ETCA), on selected core samples from a deep-water pre-salt reservoir in Brazil. This program is a first stage of a larger program to characterize the pre-salt heterogeneous reservoirs with complex fluids, including most of the elements of Advanced SCAL techniques and methods listed above. The program was aimed at measuring relative permeabilities (relperms) and capillary pressures (Pc), using carefully selected and prepared model fluids, while the next steps in the program are planned to include live fluid experiments (not covered in this article).

The key steps in the (high-level) protocol are listed here:

- Core plug and fluid selection – a collaborative effort together with Geologists, Petrophysicists, Reservoir Engineers from the asset, on basis of representativeness for flow and least heterogeneity.
- Cleaning – a detailed pre-cleaning study was executed to choose the optimal solvent able to effectively clean, while preserving the rock matrix integrity, including the solid hydrocarbon
- Samples characterization: CT scanning (using both Medical CT and micro-CT), SEM, mineralogy by X-ray Diffraction (XRD).
- Basic property measurements: ambient and stressed porosity, (Klinkenberg corrected) air permeability, grain density
- Sample saturation with (synthetic) formation brine to keep the major/key ions and match the TDS.
- Plug initialization, performed by porous plate drainage using the pressure equilibrium method, to ensure that micro pores are properly filled by hydrocarbons and representative initial water saturations (Swi), uniformly distributed across the samples are achieved.
- Ageing of samples for wettability restoration, using crude oil from the reservoir.
- Wettability evaluation performed by Amott spontaneous imbibition tests
- Unsteady-state (USS) coreflooding experiments to describe water/gas displacement and to extract relative permeability, especially the end point permeability and saturation. These are most relevant if assumption of water-wetness is accurate.
- Steady-state (SS) coreflooding experiments to describe water/oil displacement and to extract full relative permeabilities. Note that, in our experience, the SS coreflood is the best technique to extract relative permeabilities for water-oil displacement processes. However, when the rock is strongly water-wet, and especially for the gas-water systems, we find that SS corefloods are very difficult to perform. We see that even the smallest fractional flow of water can lead to a very long tail of production, dominated by spontaneous imbibition, which can last even weeks, after which there is almost no production at the subsequent fractional

flows. This makes the SS technique very impractical, and we find that USS corefloods are easier to execute and extract the key information – i.e. the end point saturation and relperms.
- Multi-speed centrifuge tests to extract imbibition capillary pressure (Pc.imb)
- Integrated data analysis and interpretation using numerical simulations with Shell in-house simulator, MoReS.

We would like to mention here that this "first stage" of the program was aimed at selecting the samples as homogeneous as possible (or more correctly, in this context, as least heterogeneous as possible) to aim as much as possible for the use of conventional/traditional SCAL 1D interpretations, while the next stages (not covered in this work) it is aimed towards the more heterogeneous samples, for which the 3D interpretation is needed.

The following subsections include detailed information related to sample preparation, cleaning and desaturation.

2.1. Sample preparation

Samples were selected carefully based on the following criteria:

- representativity for flow – based on geological core description
- rock type/facies coverage
- as homogenous (i.e. as least heterogenous) as possible, to ensure that conventional interpretations are still valid

Medical-CT images at 600 μm resolution and micro-CT images at higher resolution (40 μm) of each plug were used to assess sample heterogeneity and connectivity in the direction of flow. Fig. 1 shows a typical medical-CT with calibrated Hounsfield Units HU [12] and Fig. 2 shows a μCT image with the grey scale value for a different sample highlighting various degrees of heterogeneity. In Fig. 1, we can see the variations in pore sizes (i.e. heterogeneity). Note that the visibility of the heterogeneity in CT images fully depends on the grey-scale settings. The legend on the right-hand side indicating the HU units. The feature remains relatively the same throughout the entire plug., i.e. the heterogeneity is "uniformly distributed" (sometimes referred colloquially as "homogeneously heterogeneous") across the plug. In this way, we avoid those plugs with features (such as high perm layers, vugs, etc.) that could potentially dominate/distort the flow.

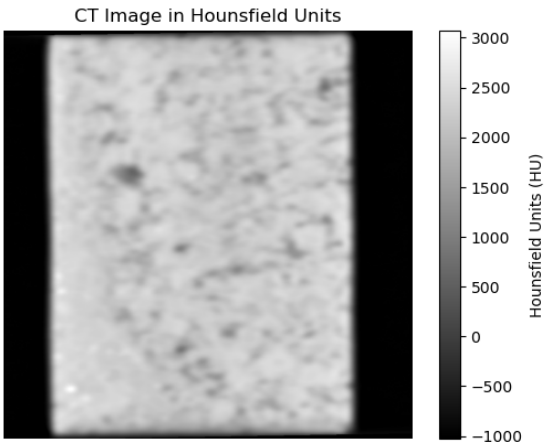

Fig. 1. Medical-CT image of one of the samples. The grey colour represents the grains, the black colour represents the pore/vugs, and white spots refer to high density inclusions.

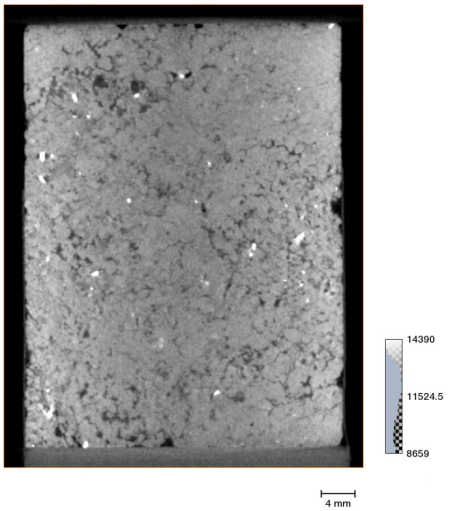

Fig. 2. Micro-CT image of one sample used for coreflooding Steady-State experiments. The grey represents the grains, and the black represents the pores and vugs. The color map legend on the right shows the range of the grey-scale value for this image. The larger number represents brighter color in the image with higher density of the material.

The porosity and permeability (at 500 psi confining stress) of the sample used in this paper are listed in Table 1.

Table 1. Porosity and permeability of the samples in this paper

Sample No.	#1	#2	#3	#4
Porosity (He)	0.18	0.09	0.10	0.09
Brine Permeability, mD	234	16	37	15

2.2. Effective cleaning

An extensive pre-cleaning study was conducted as part of the program, to ensure the optimal cleaning solvent is selected for this type of core samples. The main concern

was that conventional solvents, routinely used for RCA and SCAL may be too aggressive and could potentially damage or even remove some of the solid hydrocarbons from the matrix. Obviously, a choice for a less aggressive solvent raises the question whether cleaning will be effective enough to remove the other contamination, such as the remaining drilling fluids and any remaining hydrocarbon fluids, and to render the sample in a water-wet condition, which is the first step towards wettability restoration.

In this study, we used multiple imaging techniques including optical microscopy, SEM, micro-CT and NMR to compare the cleaning effectiveness of four solvents typically used (toluene, chloroform, tetrahydrofuran THF, and methanol) and of an additional one, cyclohexane less often used, but believed to be the least aggressive of this selection. We first picked representative plugs containing solid hydrocarbons, based on optical microscopy. Please note that all the samples used in this study were drilled from a recently drilled core, being maintained properly when handling and characterizing it. Five mini-samples with 4 mm diameter were then drilled from the selected plug and tested for the five selected solvents.

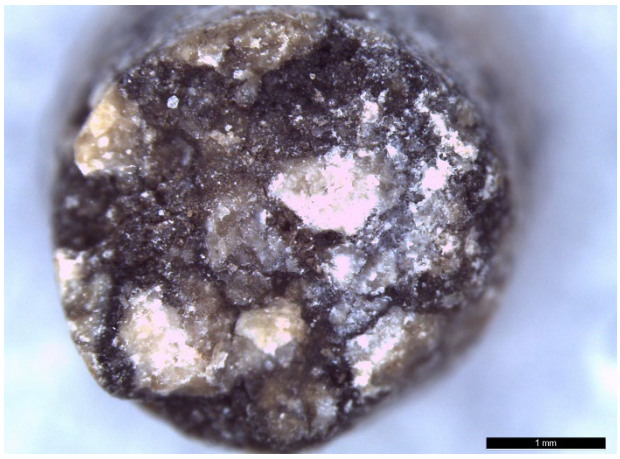

Fig. 3. A high-resolution microscopy photo of the end-face from one of the samples with a high amount of solid hydrocarbons (shown in black)

The samples were first imaged by four different methods: high resolution optical microscopy, SEM, µCT and NMR, and then put into solvents separately, for Soxhlet cleaning. The effluent was monitored regularly using Ultra-Violet (UV) fluorescence to assess the cleaning progress, until the sample was deemed to be clean. Then, samples were dried (using conventional vacuum ovens) and imaged using the same methods described above. Fig. 4 shows the effluent after extraction with 5 different solvents. From the darkness of the effluent, methanol and cyclohexane are found to be the least aggressive solvents. Fig. 5 shows images or signatures of solid hydrocarbons under the four different imaging techniques. For instance, the bitumen/solid hydrocarbons appear in µCT images with a darker grey colour, while the NMR signature is a bright off-diagonal feature in the T1-T2 spectra.

Fig. 4. The effluent after extraction with different solvents.

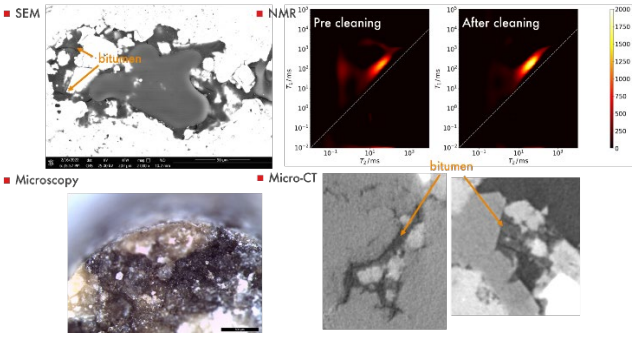

Fig. 5. Solid hydrocarbons under different imaging techniques.

After cleaning the samples in various solvents, they were immersed in Carbon Disulfide (CDS). CDS is a powerful solvent capable of removing nearly all residues from the samples. If solid hydrocarbons remained after the initial cleaning, the solvent would appear dark. Fig. 6 illustrates the cleaning results with CDS. Initially, the samples were left in the solvent for approximately 580 hours to ensure thorough cleaning. This was confirmed by the solvent's colour in the second stage, which appeared transparent after 100 hours. It is evident that the sample cleaned with cyclohexane retained the most solid hydrocarbons, followed by the sample cleaned with methanol.

The next step was to take two pieces of solid hydrocarbon (bitumen) from the samples, embed them in cyclohexane and methanol for soaking. SEM imaging was used to assess how well the solid hydrocarbons were preserved after soaking. Fig. 7 shows the effect of cyclohexane, while Fig. 8 shows the effect of methanol. Clearly there are (small) cracks on the surface of solid hydrocarbons after soaking with methanol, while they appear intact after soaking by cyclohexane.

Based on these findings, the decision was made to perform cleaning with cyclohexane, which was proven to be the least aggressive solvent, able to preserve the solid hydrocarbon in the plugs.

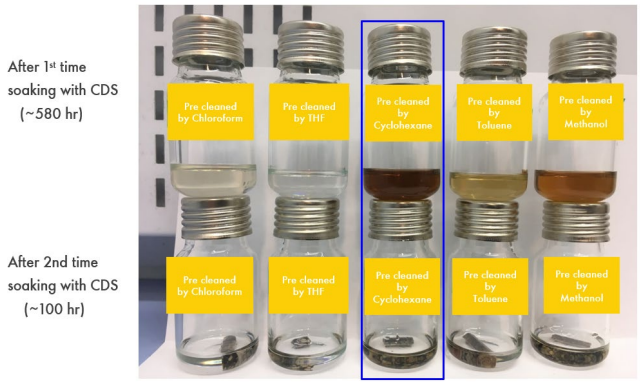

Fig. 6. The solvents of the 5 mini-samples after cleaning by CDS. Top: How the solvents look like after first soaking with CDS around 580 hours. Bottom: How the solvents look like after second time soaking with CDS around 100 hours.

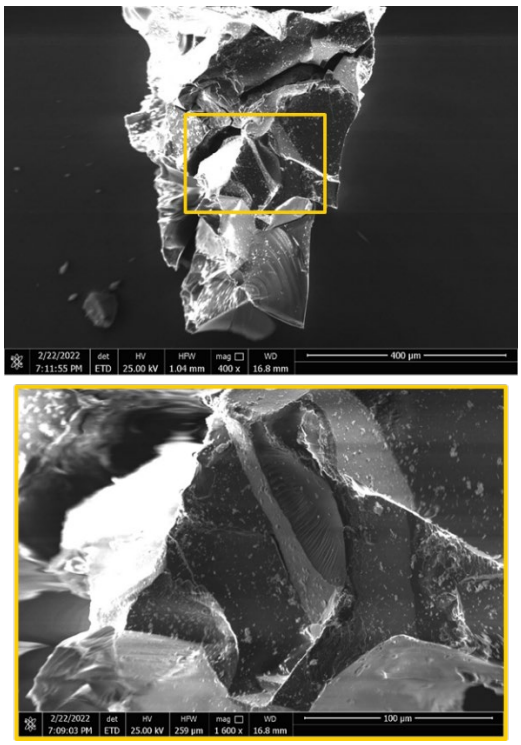

Fig. 7. Solid hydrocarbons after soaking by cyclohexane. Top: overview of this piece of solid hydrocarbons. Bottom: Zoom-in image of the yellow square part.

2.3. Desaturation/initialization to S_{wi}

After cleaning, drying and measuring basic properties (ambient and stress porosity, grain density, air permeability), the samples were saturated with formation brine and then brine porosity, brine permeability, formation resistivity factor and cementation factor were measured, at representative stress conditions. The NMR technique was used to independently assess the brine pore volume and compare it against weight based or He based values.

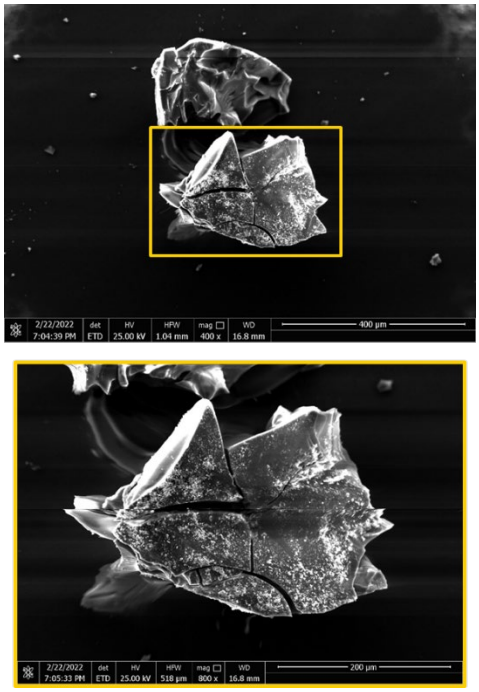

Fig. 8. Solid hydrocarbons after soaking by methanol. Top: overview of this piece of solid hydrocarbons. Bottom: Zoom-in image of the part in yellow box.

Once we ensured that all data and diagnostics shown a consistent and reliable picture, we moved to the next important step, the initialization of the samples to the representative connate water saturation. The most commonly used methods in the industry are desaturation by porous plate, centrifuge, and coreflooding, in which hydrocarbons are displacing the formation brine. In our view, the most reliable method, which provides representative S_{wi} values, uniform across the length of the plugs, is the porous plate method, when used with individual core holders, at representative reservoir confining stress. The drainage was executed either with gas (compressed air) or with oil (mineral/lab oil) and it was done slowly using the pressure equilibrium method, to ensure that there was no by-passing when filling the micropores, during the process. For most of the samples the desaturation took 9-12 months, depending on the sample permeability and pore structure. Note that the pressure steps and target S_{wi} were defined based on Mercury Injection Capillary Pressure (MICP) tests performed prior to the start, on trim ends of the samples. S_{wi} is ranging from 0.1 to 0.4. For the oil samples, after porous plate drainage was completed, crude oil was injected into plugs to displace the lab oil at reservoir temperature for ageing. The plugs were kept in crude oil and aged for 4 weeks [15]. The gas samples were directly used for the next steps without ageing.

3. Measurements, Results, Discussions

In this section we will discuss in detail the main experiments performed in the program, focusing on spontaneous imbibition, coreflood and centrifuge tests.

3.1. Spontaneous imbibition tests

Spontaneous imbibition tests were performed on multiple unaged samples, with water imbibing against gas. The objective of the tests was to obtain insights into wettability of the reservoir rock, especially for the process of water displacing hydrocarbons. The tests were performed on samples at S_{wi}, at ambient temperature and pressure conditions, in a conventional Amott tests cell, using formation brine for water and air for gas. When a core plug is placed in formation water depending on the wettability, water would imbibe spontaneously into the plug, while the gas would be produced and captured at the top of the cell. From the gas production, saturations in the plug can be calculated. At the end of the tests, the weight of the samples was carefully measured to confirm material balance, a key step, especially important for imbibition against gas.

Fig. 9 shows a typical test in which the gas saturation in the sample is shown as function of time. All samples have showed a similar behaviour, with a relatively quick but small decrease of Sg (most of it in the first day), followed by a very slow but also very limited decrease afterwards. After almost a month, the samples gas saturation was still in the range of 0.7 – 0.8, indicating a rather small amount of imbibition, resulting in a high remaining gas saturation (RGS). Give the high value of RGS, it is unlikely, in our view, that the RGS is close to the trapping saturation (S_{grw}). Clearly, this is indicating a non-water-wet behaviour, even though the fluid used in this test was air.

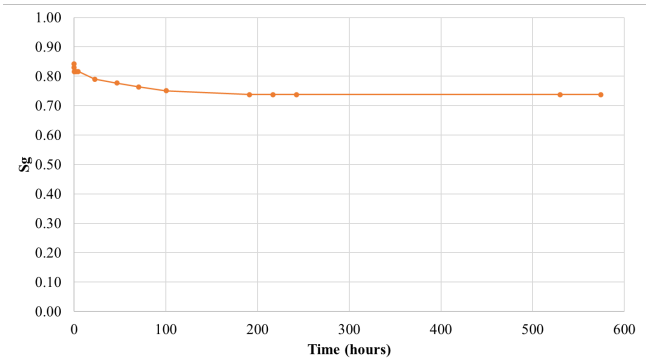

Fig. 9. Typical production curve during Amott spontaneous imbibition test.

3.2. Unsteady state (USS) coreflooding tests

The next step in the program was to perform coreflooding experiments using brine displacing gas. The main objective of the experiments was to further test the non-water wetness hypothesis proposed to explain the spontaneous imbibition tests and to extract relative permeabilities and trapping saturations. As it is well documented in the literature [13], the most reliable corefloods for water/gas displacement are the low-rate USS coreflood tests. We, therefore, decided to perform several such tests on our pre-salt carbonate samples. These coreflood experiments are challenging because of the high gas compressibility, dissolution and diffusion effects which could, if not carefully executed, lead to numerous experimental artefacts (e.g. permeability and saturation measurements could become inaccurate). To mitigate for that, based on in-house expertise and in agreement with industry standards, the coreflooding experiments were performed starting at low flow rates, of ~ 0.05 ml/min [13,14]. Moreover, we executed the tests in experimental set-ups with low dead volumes and with simultaneous measurements of gas production, directly by an accurate weighing unit, at the outlet of the sample and indirectly, by in-situ saturation monitoring (ISSM) with X-ray absorption.

The experiments were started at low flow rate (~0.05 ml/min) for a few injected PV until pressure and production profiles were deemed to be stable. After that, in line with our internal protocols, the flood rate was increased in steps, to check whether capillary end effects played a role and (in case they were present) to minimize this experimental artefact. At each step pressure, production and saturation profiles were carefully monitored until stable readings for both was achieved. Calibration of the ISSM X-ray attenuation data was performed at the end of the tests, while keeping the sample in the set-up, cleaning it and measuring the 100% brine and 100% hydrocarbon absorption.

After the tests, gas production and pressure drop over the samples as function of time, and saturation profiles across the length of the samples were carefully analysed for consistency. We assessed whether the shapes of the profiles and their absolute or relative values were aligned with expectations. Analytical methods for estimating S_{grw} and $K_{rw}@S_{gr}$ (residual gas saturation and endpoint relative permeability to water) were used for a quick assessment. As an example, Fig. 10 shows the production profiles (pressure drop over the sample, dP, and average water saturation, $S_{w,avg}$) for one of the samples. One can see that both dP and $S_{w,avg}$ have been stable for at least 6 hours before the next flow rate was applied. We can see the gas production increased each time when a higher flow rate was applied. Fig. 11 shows the saturation profiles at different flow rates. Overall, the saturation profiles show that there is a decrease of S_w at the end of the sample, confirming that the capillary end effect (Pc-end effect) is present in the sample, which a hallmark of non-water behaviour. Moreover, the incremental production as the injection rate was increased (therefore higher viscous pressure drop) was partially due to the reduction in this Pc-end effect. We also note that although the saturation profiles suggest a typical Pc-end effect, it cannot be ruled out that the Pc-end effect is possibly enhanced by the heterogeneity. The fluctuations in saturations along the sample also indicate the impact of local heterogeneity.

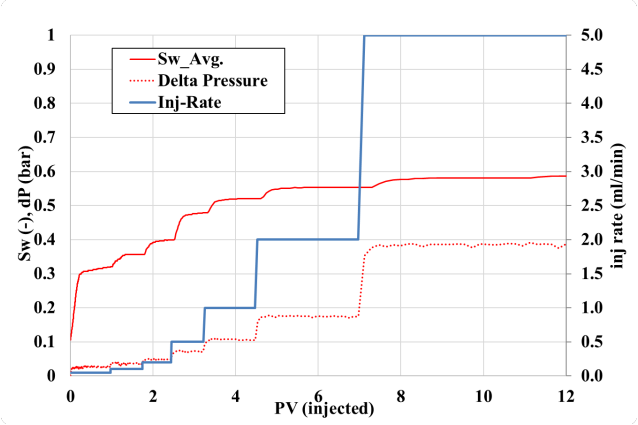

Fig. 10. USS coreflood test process for sample #1, including average water saturation, injection rate and pressure drop.

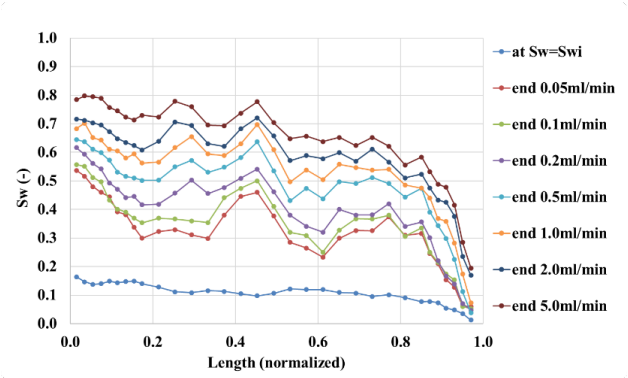

Fig. 11. USS coreflood test saturation profiles at different flow rates for sample #1.

3.3. Steady state (SS) coreflooding experiments

Given the fact that the reservoir rock showed clear indication of non-water wet behaviour, we decided to proceed with the next phase of the program. Steady-State (SS) water/oil coreflooding tests were performed on core plug samples, which were prior to that, desaturated by porous plate and aged with crude oil. The main objective of the tests was to extract representative water/oil relative permeabilities, after restoring the wettability.

The tests execution followed Shell in-house protocols. At first, X-ray scans and permeability measurements were performed at irreducible water saturation. Formation brine and oil were simultaneously injected in the core at the specified oil to brine flow rate ratios (fractional flows of oil: water of 100:0, 98:2, 95:5, 90:10, 80:20, 60:40, 40:60, 20:80, 10:90, 5:95, 2:98, 1:99, 0:100). At each step pressure, production and saturation profiles were carefully monitored. Note that we have used more fractional flow steps than we normally do for typical SS corefloods, to more accurately capture potentially large variation in pressure (and implicitly in relperms) for relatively small Sw changes. The saturation distribution was extracted by X-ray scanning of the core-plug the at appropriate time intervals, similar to the procedure described in section 3.2. Flowing of brine and oil through the core was continued until the pressure drop and the average saturation over the core-plug were stable. At least one bump flow rate at 100% water injection was applied to displace additional oil and get as close as possible to S_{or}. In the case shown in Fig. 14, three bump flood rates (0.4 mL/min, 1 mL/min and 2 mL/min) were used to try to reduce the Pc-end effect and to get closer to the trapping oil saturation. Calibration of the ISSM X-ray attenuation data was performed at the end of the tests, in the same way described in section 3.2.

Fig. 12 shows a typical example (in this case, for sample #2) of the production profile for the SS coreflood, i.e. pressure drops over the sample and average water saturation, as function of time, at each fractional flow. The decision to move to the next fractional flow was made only after ensuring that the average water saturation and pressure drop were stable enough. Note that the criterion for stability was a variation of less than 0.002 bar/hour (for pressure) and 0.05%/hour (for the saturation) in the last 6 hours.

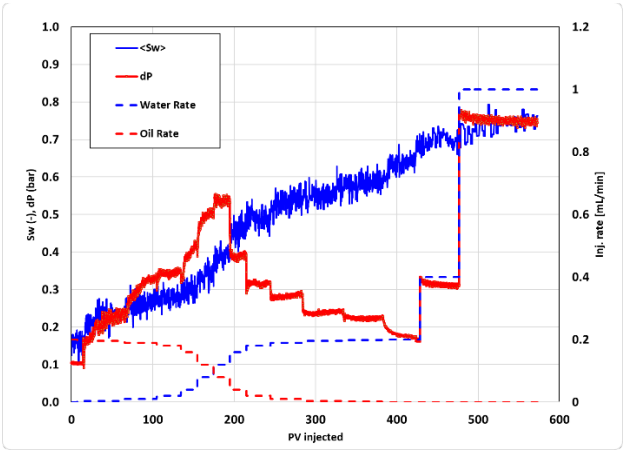

Fig. 12. SS coreflood profiles (pressure drop in red, average saturation in blue vs. PV injected, water rate and oil rate) for sample #2.

Fig. 13 shows the water saturation profiles across the sample#2, at the end of each fractional flow. We observe significant S_w fluctuations, especially at the low fraction flow of water. We associate these fluctuations with the heterogeneity of the pre-salt carbonates. Interestingly, these fluctuations become smaller at the high fractional flow, especially after applying the bump floods. This indicates that with increasing the water flow rate the pores are more uniformly flooded than at low fractional flows.

To better illustrate this effect, we show in Fig. 14 another example (sample #3) for which the saturation profiles along the sample show less fluctuations, which are more aligned with a typical SS test. We can see a large saturation change from S_{wi} to the first ratio. Relatively smaller change in intermediate ratios. Profile changes during final 100% water injection and the bump flood.

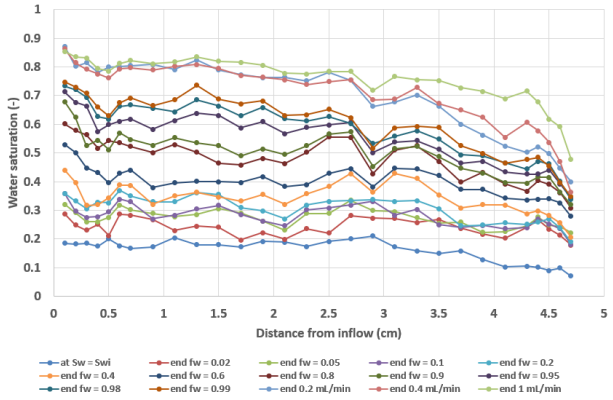

Fig. 13. SS saturation profiles along the sample for sample #2, measured by ISSM at the end of each fractional flow step.

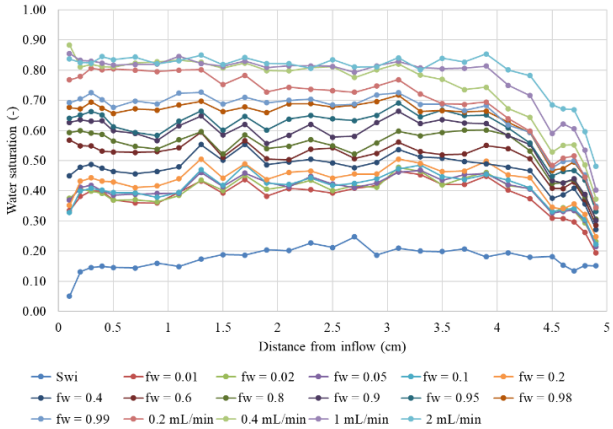

Fig. 14. SS saturation profiles along the sample for sample #3, measured by ISSM at the end of each fractional flow step.

3.4. Imbibition capillary pressure centrifuge experiments

Multi-speed imbibition centrifuge (MSC) measurements were performed in parallel on samples with similar properties with the ones used for coreflooding. The main objective was to measure the imbibition capillary pressure, which is necessary for the more robust interpretation of the USS and SS coreflooding tests [16]

Samples were put in the ultra-centrifuge set-ups, in cups surrounded with brine and preheated to the target measurement temperature. The centrifuge was spined at 8-10 speeds and production was accurately recorded with automated data acquisition camera. The decision to proceed from one speed to the next was only taken if the production profile was found to be stable enough. Note that the criterion for stability was a variation of less than 0.005 mL/hour in the last 6 hours. This implies that for lower permeability samples it required multiple days per centrifuge speed. At the end of the test the sample weight was recorded, as well as the effluent brine volume, to check the material balance. The capillary pressure (*Pc*) was calculated from centrifuge production data using the analytical Hassler-Brunner method [17] or numerical simulations. The absolute value of Pc was quite high, but did not exceed the critical Bond number of 10^{-5}, even though we believe that the critical Bond number can be higher than 10^{-5} for non-water-wet system [18]. Fig. 15 shows a typical imbibition capillary pressure (Pc.IMB) curve derived analytically, using Hassler-Brunner method.

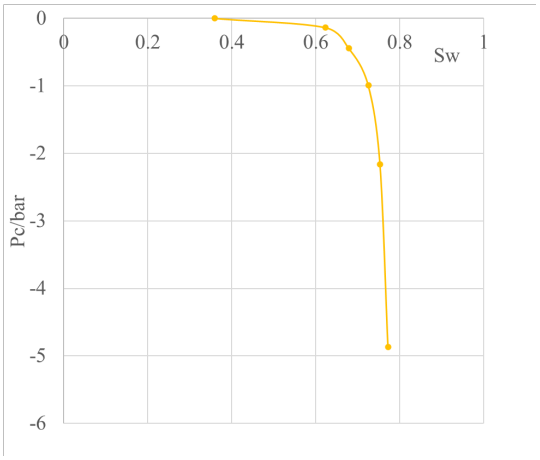

Fig. 15. Imbibition capillary pressure (Pc.IMB) curve for sample #4 estimated analytically by Hassler-Brunner method.

3.5. Numerical simulations

After completion of the tests, numerical simulations were performed to history match the experiments and to extract parameters such as relative permeability. We show below an example of such numerical simulations applied to the SS coreflood experiments. A 1D numerical model was built using the Shell in-house simulator MoReS, for data interpretation. 50 grid blocks were set along the flow/displacement direction (the Z direction, corresponding to the vertical direction of the flow during coreflooding test). Sample dimensions, porosity, absolute permeability, as well as fluid properties were honoured.

The matching to the measured data was done manually with iterations. We selected sample pairs with comparable permeability and porosity for each pair - one was used in SS corefloods and one in centrifuge. Note that there are no true twin plugs due to the local heterogeneity. Initially, we began with analytical relative permeability and imbibition Pc from centrifuge tests, as initial inputs. Residual oil saturation Sor from imbibition Pc is honoured in SS test, unless saturation profile indicated a much lower or higher Sor. In that case, we consider that the imbibition Pc on that plug is not representative for the plug used for coreflooding. Also, for these samples the initial water saturation Swi is very much dependent on the exact pore size distribution for each sample. When differences are seen between the coreflood sample and its pair used for the centrifuge test, we honour the Swi from the coreflood test. The relperms and Pc were adjusted to match the measured pressure, the average saturation and the saturation profiles

manually, until all experimental data are satisfactory matched [19]. The match is considered satisfactory when there is a good overall match of the dP, S_w.avg and S_w profiles. In practice it is impossible to get a perfect match of all points. We put more emphasys on matching the stable part of the dP and S_w.avg, as it is clear that the transient part may be more impacted by other factors, including heterogeneity.

Fig. 16 shows the match for time dependence of pressure drop and Fig. 17 shows the match for the saturation profiles along the sample #2. In the history matching of corefloods, it is essential to handle boundary conditions in a manner that accurately reflects laboratory conditions. This was emphasized in a comparative study by Lenormand et al. [20], which demonstrated the importance of incorporating additional grid blocks to account for the influence of grooves in the end flanges of experimental setups. For boundary conditions, extra grid blocks were added with Pc=0 to represent the fluids in the first and last grid block just outside the plug. Measuring the pressure drop (ΔP) in the simulator between these extra grid blocks provides a more appropriate basis for comparison with laboratory ΔP data. This approach also eliminates the need for a subjectively defined switch-point between using ΔP in the water or oil phase.

The relative permeabilities for sample #2, extracted from the SS coreflood are shown in Fig. 18, using both the linear plot (top) and the semi-log plot (bottom). For comparison, we plotted on the same graphs the analytical solution (which assumes Pc = 0) and the numerical simulation solution obtained from the (manual) history matching. At low water saturations ($S_w < 0.4$), where the Pc curve is small, the differences between the two solutions are small, as expected. At higher water saturations, where the Pc is larger, the capillary end effect plays an increasingly important role and the differences between $S_{w,avg}$ and S_w at each position in the sample becomes large. As a result, not unexpectedly, we see significant differences between the two results. Both the k_{rw} and k_{ro} show shapes that are very difficult to fit with correlations commonly used in the industry. For reference we plotted the Corey correlation curves, and the Corey modified curves (see [20]), the latter being able to capture a larger Sw range, but not the whole range.

Fig. 19 shows the initial input data for imbibition Pc, in red (based on the multi-speed centrifuge data measured on sample #4), and the Pc estimated from history matching in green, showing some differences across the Sw range (higher in absolute magnitude at lower S_w and lower at high S_w). For reference, the quality of the history matching of the centrifuge test is shown in Fig. 20.

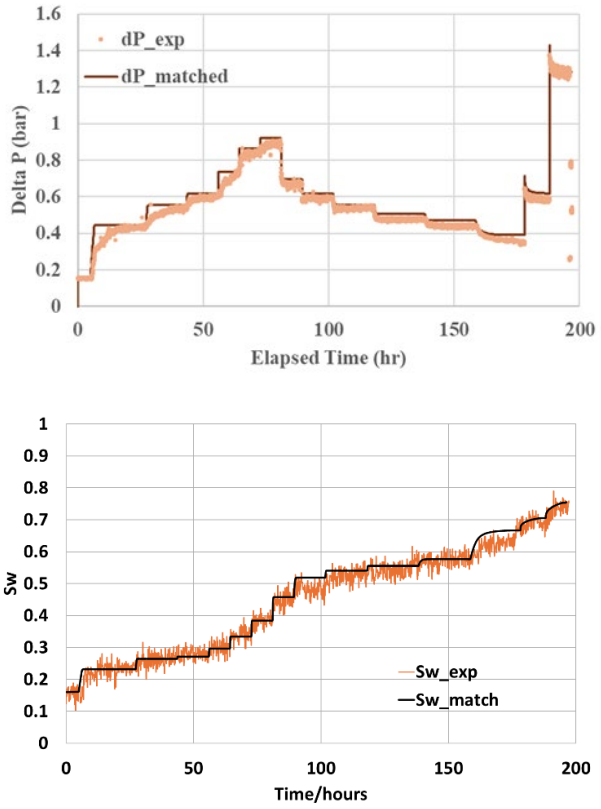

Fig. 16. SS coreflood production profiles (top: pressure drop vs. time, bottom: average saturation vs. time) for sample #2, showing experimental data and the history matching.

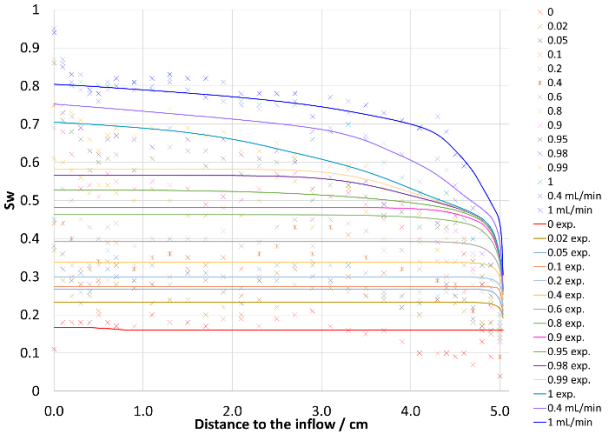

Fig. 17. SS saturation profiles history match along the sample for sample #2.

3.6. Discussion of results

It is clear from all experimental data that the samples are non-water-wet, in spite of the fact that the reservoir hydrocarbon fluids are rich in light components. The first step of the program, which consisted of Amott spontaneous imbibition tests, showed only a small amount of spontaneous imbibition, even though we used gas (compressed air), known as being the least wetting phase, in combination with brine.

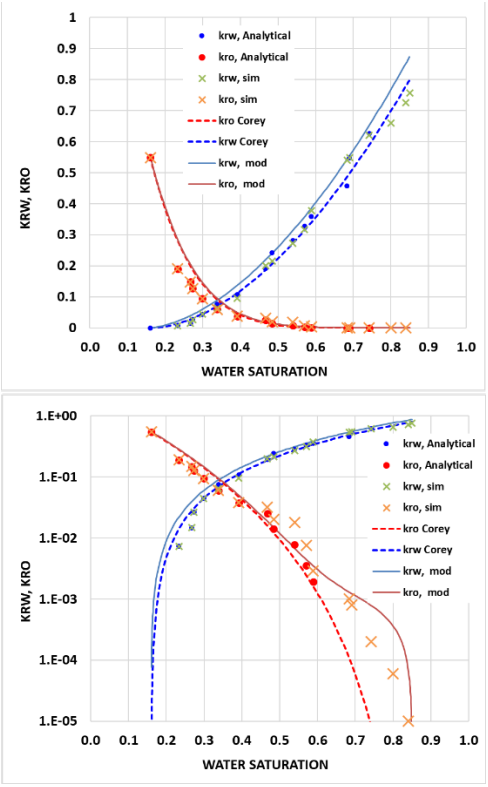

Fig. 18. Relative permeabilities for sample #2 - linear plot (top) and semi-log plot (bottom). For comparison we show the analytical solution, the numerical simulation solution (history matching). The Corey curves and the Corey modified curves [21] are shown as indication of difficulty to fit them with industry used corelations.

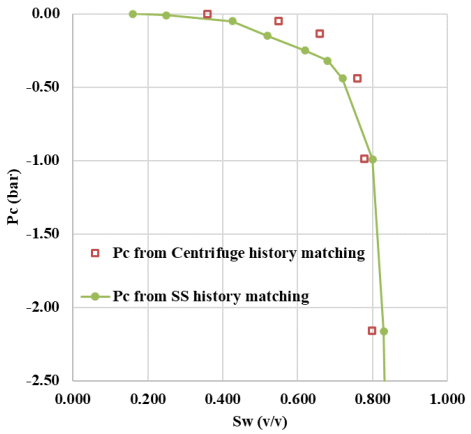

Fig. 19. Comparison of imbibition Pc, used for the best fit during history matching (green) of sample #2, and the Pc from centrifuge history matching, on an analogue sample #4 (red).

The USS corefloods, in which the production was simultaneously measured by with X-ray absorption based ISSM and by production shows clear indication of the non-water wet behaviour: at each increase of the flow rate, we observe significant extra production. In the water-wet case, sample reaches trapped saturation already at breakthrough, not requiring any additional bump floods. In contrast, in a non-water-wet case, bump floods (of higher flow rates) are required to approach the trapping saturation.

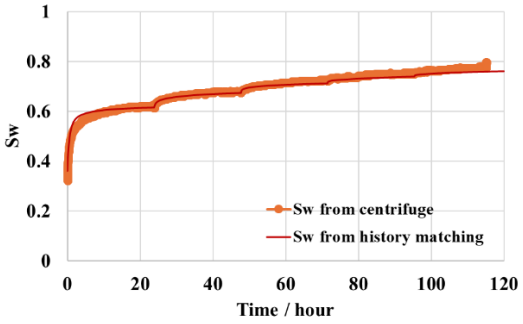

Fig. 20. Centrifuge production profiles for sample #4, showing experimental data and the history matching.

The SS corefloods confirm this wettability hypothesis. The saturation profiles show, for all samples, significant Pc-end effects, at the outlet. In addition, the bump floods performed at the end of the tests, lead to significant extra production, by reducing the magnitude of the P_c-end effect. Moreover, the relative permeabilities, extracted from numerical simulations, show significant drop in oil relperms (k_{ro}) already close to connate water S_{cw}, with only a small increase in S_w, while the end points water relative permeability (k_{rw}') are relatively high. All these provide a consistent and systematic picture with respect to the non-water nature of wettability.

A key question is, obviously, what would be the cause for fluids are rich in light components to exhibit non water wet behaviour. Our interpretation is that the presence of significant amount of solid hydrocarbons possessing polar component adhered to the pores is responsible for establishing wettability between the hydrocarbons and the rock matrix, that otherwise would be difficult, if not impossible to form for light oil components.

Another important element is, of course, the heterogeneity, especially the fact that it is present at small scale, which is a key characteristic of these pre-salt carbonates. This makes it very difficult to find core plug samples that are sufficiently homogeneous, which has been traditionally one of the important requirements of core analysis, especially for measurements that rely entirely on volumetric measurements. To mitigate for that, it is, therefore, very important that the coreflooding experiments are performed using in-situ saturation monitoring during flooding. As expected, both the USS and SS corefloods performed on these pre-salt carbonates show that the saturation, extracted from ISSM by X-ray absorption, show significant fluctuations. In general, we observe that the fluctuations are significantly higher in amplitude for USS test, when compared to SS tests. A typical difference is illustrated by comparing Fig. 14 (SS test) with Fig. 11 (USS test). By exception, however, we also encountered a case (sample #2, shown in Fig. 13) for which there are large fluctuations during SS corefloods, as well. Without ignoring this outlier (sample #2), we would like to stress that is our general experience that the SS corefloods are

less impacted by the effect of heterogeneities than the USS corefloods and, therefore, tend to provide results that are more robust (see also [22]).

We notice that the variation in saturation, at lower values of S_w, could be amplified by the fluid distribution (due to heterogeneity). At higher water fractional flows (for SS tests) and at higher flow rates (for both USS and SS, bump floods) the amplitude of fluctuations is decreasing, indicating that the saturation profiles across the samples are less impacted by the presence of heterogeneities. This is reassuring as it means that the higher end of the water saturation range for relative permeabilities and the remaining/residual hydrocarbons saturations can be estimated in a more robust manner, and it is less sensitive to the degree of heterogeneity in the sample. For the intermediate range of saturations, for which the fluctuations are quite significant, both the k_r values and the Sw values show larger error bars. See for instance the curves and the associated error bars in Fig. 18.

Last but not least, given the significant role played by the heterogeneities and the fact that their impact varies in magnitude across the saturation range, we cannot exclude that there is interplay between the wettability (non-water wet nature) and the gradual filling of local heterogeneities, which cannot be easily separated at this stage, especially in this first phase of the program, in which we have only used 1D in situ saturation. For the next phases of the program there are already ongoing efforts to use 3D ISSM to characterize the heterogeneity in pre-salt carbonates to more accurately separate the two effects [6,9].

4. Summary and Conclusions

In this paper we presented the first phase of a detailed core analysis program focused on extracting relative permeabilities and capillary pressures for pre-salt carbonates. These reservoirs bring several key challenges. The reservoirs are highly heterogeneous, with large variations in porosity and permeability, often contain significant amounts of solid hydrocarbons inside the pores or on the pore throats, and the fluids are, often, rich in light components. The core analysis requires the application of Advanced Special Core Analysis (SCAL) techniques and integrated workflows

In the Shell Rocks & Fluids laboratory in Amsterdam, we combined innovative technologies, including imaging with μCT, NMR/MRI, SEM in combination with coreflooding performed using in-situ saturation monitoring (ISSM), to obtain reliable fluid flow parameters such as relative permeability, capillary pressure, trapping saturation values.

The SCAL workflow used was described in detail and it included a careful selection of the samples, characterization using a multitude of techniques, and a pre-cleaning study on selecting the most optimal solvent for effective cleaning (while preserving the integrity of the reservoir rock, including of solid hydrocarbons). The selected solvent was cyclohexane, which was the least aggressive while still effective in cleaning the samples. Plug initialization was performed by porous plate drainage using the pressure equilibrium method, to ensure that micropores are properly filled by hydrocarbons and representative initial water saturations (S_{wi}), uniformly distributed across the samples are achieved. Ageing of samples, using crude oil from the reservoir.

The first pass wettability evaluation was performed using the Amott spontaneous imbibition tests for a pair of gas/brine fluids. These tests were followed by water/gas USS coreflooding experiments and brine/oil SS coreflooding experiments, to extract relative permeability and multi-speed centrifuge tests, to extract imbibition capillary pressure. The X-ray based ISSM played a key role in execution and interpretation of the coreflooding tests. All experimental tests were history matched using in-house numerical simulations tools and techniques, in order to accurately interpret the results. We found a very consistent and systematic picture, indicating that the reservoir rocks are non-water wet, in spite of the fact that the reservoir hydrocarbon fluids are rich in light components, which is usually linked to water wetness. We believe (similar to observations made in [10]) that the non-water wetness is caused by the presence of significant amounts of solid hydrocarbons inside the pores and along pore throats. The small-scale heterogeneity, present at core plug scales, made the sample selection, execution of the tests and their interpretation challenging. The use of ISSM was key and we found that the saturation profiles were more significantly impacting the relative permeabilities in the mid saturation range, rather than the end point range, which was less sensitive to the local heterogeneities. We also observed less impact on SS corefloods compared to USS corefloods, making, in our view, the SS tests more reliable.

We recognize that in order to better understand and separate the effect of heterogeneities on the wettability assessment we would need to move from 1D to 3D in situ saturation, which are currently progressing in the next phase of the program.

We would like to thank Steffen Berg and Matthias Appel for insightful discussions and Shell Brasil Petroleo Ltda. and Shell Brasil Subsurface and Exploration for permission to publish the data.

References

1. V.D. Chitale, G. Alabi, P. Gramin, S. Lepley, and L. Piccoli, *Reservoir Characterization Challenges due to Multiscale Reservoir Heterogeneity in the Pre-*

Salt Carbonate Sag Formation, North Campos Basin, Brazil, Petrophysics 56 (6), 552-576 (2015)

2. A.C. Azerêdo, L.V. Duarte, and A.P. Silva, *The challenging carbonates from the Pre-Salt reservoirs offshore Brazil: facies, palaeoenvironment and diagenesis*, Journal of South American Earth Sciences, 108, 103202 (2021)
3. R.A.M. Vieira, M.A. Cardoso, and J.O.S. Pizarro, *An Integrated WAG Characterization Study for an Offshore Oilfield,* OTC-29766-MS, presented at the Offshore Technology Conference Brasil, October 29–31, 2019 (2019).
4. F. Bordeaux-Rego, J. A. Ferreira, C. A. S. Tejerina, and K. Sepehrnoori, *Modeling Oil Recovery in Brazilian Carbonate Rock by Engineered Water Injection Using Numerical Simulation*, Energies, 14 (11), 3043 (2021).
5. T. Ramstad, A. Kristoffersen, L. Rennan, R. Wat, and C.J.T. De Lima, *Micro-CT Imaging of Low Salinity Water Induced EOR Mechanisms in Pre-Salt Carbonates*, presented at the 2nd EAGE Conference on Pre-Salt Reservoir, vol. 2021, pp.1-5 (2021).
6. S. Drexler, A. Fadili, Y. Wang, T. Yeh, B. Roussenac, and S. Berg, *Pre-Salt Carbonates Relative Permeability Characterization: 3D Digital Workflow for Numerical Interpretation*, presented at the 4th EAGE Conference on Pre-Salt Reservoir, Vol. 2024, No. 1, pp. 1-6 (2014)
7. I. Abu-Shiekah, S.K. Masalmeh, and X.D. Jing, *Experimental investigation and modelling of waterflooding performance of a bioturbated carbonate formation*, SCA2007-19, presented at the SCA Annual Symposium, Calgary, Canada, 2007 (2007).
8. O. Karoussi, R.M.S. Wat, C.D. Lima and L. Ribeiro, *Potential wettability alteration/IOR study for pre-salt carbonate by low salinity brines: from experiments to field scale simulation*, SCA2024-1046, presented at the SCA Annual Symposium, Montreal, Canada, August 2024 (2024).
9. Y. Wang, and S.V. Galley, *Impact of Dual Matrix Porosity in Sandstone on Fluid Distribution and Flow Properties*, Petrophysics, 66 (1), 135-154 (2025).
10. W.J. Looyestijn, J.L. Alixant, and J.P. Hofman, *Unusual Logs in an Unusual Formation: NMR in Athel Silicilyte*, SPE 50600, presented at the SPE European Petroleum Conference, The Hague, The Netherlands, 20–22 October 1998 (1998).
11. Y. Wang and S.K. Masalmeh, *Obtaining High Quality SCAL Data: Combining Different Measurement Techniques, Saturation Monitoring, Numerical Interpretation and Continuous Monitoring of Experimental Data*, SCA2018-015, presented at the SCA Annual Symposium, Trondheim, Norway, August 2018 (2018).
12. J.G. Maas and A. Hebing, *Quantitative X-ray CT for SCAL plug homogeneity assessment,* SCA2013-004, presented at the SCA Annual Symposium, Napa Valley, California, USA, September 2013 (2013).
13. A.W. Cense, J. Reed, and P. Egermann, *SCAL for gas reservoirs: a contribution for better experiments, SCA2016-023*, presented at the SCA Annual Symposium, Snowmass, Colorado, USA, 21-26 August 2016 (2016).
14. Y. Gao, T.G. Sorop, N. Brussee, H. van der Linde, A. Coorn, M. Appel, and S. Berg, *Advanced Digital-SCAL Measurements of Gas Trapped in Sandstone*, Petrophysics 64, 368–383 (2023).
15. J.A. Kokkedee and V.K. Boutkan,*Towards Measurement of Capillary Pressure and Relative Permeability at Representative Wettability*, proceedings of the 7th European IOR Symposium, Moscow, October 1993 (1993).
16. S.K. Masalmeh and X.D. Jing, *The importance of Special Core Analysis in modelling remaining oil saturation in carbonate fields*, SCA2008-003, presented at the SCA Annual Symposium, Abu Dhabi, October 2008 (2008).
17. G.L. Hassler and E. Brunner, *Measurement of Capillary Pressures in Small Core Samples*, SPE 945114, Trans. AIME, 160, 114, Arlington, Virginia, USA (1945).
18. K. J. Humphry, B. M. J. M. Suijkerbuijk, H. A. van Der Linde, S. G. J. Pieterse, and S. K. Masalmeh, *Impact of wettability on residual oil saturation and capillary desaturation curves.* Petrophysics, 55(04), 313-318 (2014)
19. J.G. Maas, B. Flemisch and A. Hebing, *Open source simulator DUMUx available for SCAL data interpretation*, SCA2011-08, presented at the SCA Annual Symposium, Austin, Texas, USA, 2011. (2011)
20. R. Lenormand, K. Lorentzen, J. G. Maas, and D. Ruth, Comparison of four numerical simulators for SCAL experiments, SCA2016-06, presented at the SCA Annual Symposium, Colorado, USA, August 2016 (2016).
21. S.K. Masalmeh, I. Abu-Shiekah, and X.D. Jing, *Improved Characterization and Modeling of Capillary Transition Zones in Carbonate Reservoirs*, SPE 109094, SPE Res Eval & Eng 10 (02): 191–204 (2007).
22. A. Zweers, W. Scherpenisse, K. Wit and J.G. Maas, *Relative Permeability Measurements on Heterogeneous Samples: A pragmatic approach*, SCA-9909, presented at the SCA Annual Symposium, Golden, Colorado, USA (1999).